Inorg. Chem. **2004**, *43*, 264–274

Oxyl Radical Required for O–O Bond Formation in Synthetic Mn-Catalyst

Marcus Lundberg,* Margareta R. A. Blomberg, and Per E. M. Siegbahn

Department of Physics, Stockholm University, AlbaNova University Center, Stockholm Center for Physics, Astronomy and Biotechnology, SE-106 91 Stockholm, Sweden

Received July 14, 2003

DFT calculations using the B3LYP functional support the suggestion that the $[(terpy)(H_2O)Mn^{IV}(\mu\text{-}O)_2Mn^{III}(H_2O)(terpy)]^{3+}$ (terpy=2,2′:6,2″-terpyridine) complex functions as a synthetic O_2 catalyst. The calculated barrier for O–O bond formation with water is 23 kcal/mol. In this complex, as well as in models of the oxygen evolving complex in PSII, the active species is a Mn^{IV}-oxyl radical. From comparisons with inactive Mn^{V}-oxo complexes, it is proposed that radical formation is actually a requirement for O_2 formation activity in Mn-complexes.

I. Introduction

In their process of solar energy harvesting, higher plants have developed the ability to form O_2 from water. This process takes place in the oxygen evolving complex (OEC) in photosystem II (PSII). Experimental data show that this is a tetramanganese complex, linked by several oxo-bridges,[1] and X-ray structures with increasing resolution are in progress.[2,3] Despite the wealth of experimental information available, the mechanism for this fundamental reaction is not yet fully understood. It is well-known that oxidation of water to O_2 takes place through a series of four one-photon, one-electron transfer steps, taking the manganese complex through the states S_0 to S_4. From S_4, O_2 is released, returning the complex to the S_0 state. However, the nature of the highly oxidized states is still unclear, as are the details of the O−O bond formation reaction.

Only a few man made biomimetic complexes can perform the task of catalytic O_2 formation from water, mainly Ru- and Mn-complexes.[4] Two truly catalytic Mn-complexes are the Mn-dimer $[(terpy)(H_2O)Mn^{IV}(\mu\text{-}O)_2Mn^{III}(O)(terpy)]^{3+}$ (terpy = 2,2′:6,2″-terpyridine)[6] and an *o*-phenylene bridged Mn-phorphyrin dimer.[5] These synthetic complexes can either be considered as early precursors for a large scale solar energy conversion system or merely as tools that can be used to increase the understanding of photosynthesis in plants.

If the goal is to increase the understanding of O_2 evolution in photosystem II (PSII), the most interesting synthetic catalyst is probably the Mn-complex $[(terpy)(H_2O)Mn^{IV}(\mu\text{-}O)_2Mn^{III}(H_2O)(terpy)]^{3+}$ (terpy = 2,2′:6,2″-terpyridine).[6] It is the active synthetic complex that is most similar to the OEC, with both complexes having Mn atoms linked by μ-oxo bridges. Due to the structural similarities, it is reasonable to believe that O−O bond formation proceeds through similar intermediates in the two complexes.

Limburg et al., who synthesized the active Mn-dimer, propose that the active state in O−O bond formation, in the synthetic complex as well as in the OEC, is the highly oxidized Mn^{V}-oxo state.[6] However, well characterized Mn^{V}-oxo complexes exist that are not active in O−O bond formation,[7−9] so formation of a highly oxidized Mn^{V}-oxo state cannot be the only requirement for O−O bond formation. The true requirements for this fundamental reaction are thus not yet known.

The goal of the present investigation is to analyze the nature of the highly oxidized species and the requirements for O−O bond formation in Mn-complexes. The tool used is density functional theory (DFT) with the hybrid functional

* Corresponding author. E-mail: marc@physto.se. Phone: +46-8-55 37 87 06. Fax: +46-8-55 37 86 01.

(1) Yachandra, V. K.; Sauer, K.; Klein, M. P. *Chem. Rev.* **1996**, *96*, 2927−2950.
(2) Zouni, A.; Witt, H.-T.; Kern, J.; Fromme, P.; Krauss, N.; Saenger, W.; Orth, P. *Nature* **2001**, *409*, 739−743.
(3) Kamiya, N.; Shen, J. R. *Proc. Natl. Acad. Sci. U.S.A.* **2003**, *100*, 98−103.
(4) Rüttinger, W.; Dismukes, G. C. *Chem. Rev.* **1997**, *97*, 1−24.
(5) Naruta, Y.; Sasayama, M.; Sasaki, T. *Angew. Chem., Int. Ed. Engl.* **1994**, *33*, 1839−1841.
(6) Limburg, J.; Vrettos, J. S.; Chen, H.; de Paula, J. C.; Crabtree, R. H.; Brudvig, G. W. *J. Am. Chem. Soc.* **2001**, *123*, 423−430.
(7) Collins, T. J.; Gordon-Wylie, S. W. *J. Am. Chem. Soc.* **1989**, *111*, 4511−4513.
(8) Collins, T. J.; Powell, R. D.; Slebodnick, C.; Uffelman, E. S. *J. Am. Chem. Soc.* **1990**, *112*, 899−901.
(9) MacDonnel, F. M.; Fackler, N. L. P.; Stern, C.; O'Halloran, T. V. *J. Am. Chem. Soc.* **1994**, *116*, 7431−7432.

10.1021/ic0348188 CCC: $27.50
Published on Web 11/25/2003

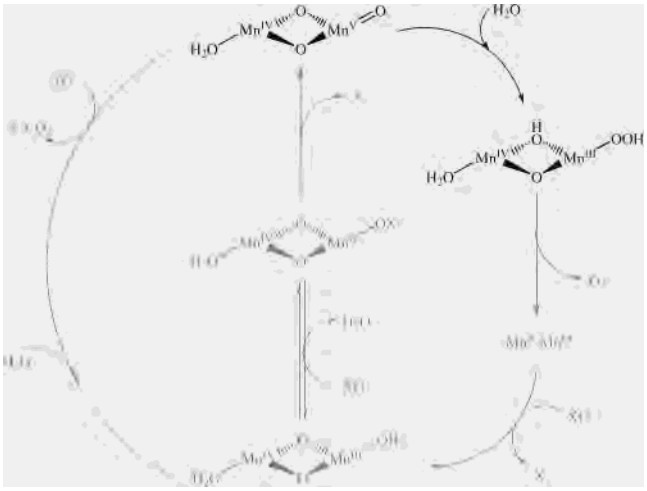

Figure 1. Reaction scheme for O_2 evolution by the Mn-dimer [(terpy)-$(H_2O)Mn^{IV}(\mu\text{-}O)_2Mn^{III}(H_2O)$(terpy)] adapted from ref 6. The present theoretical study focuses on the species and the reaction step shown in black, the O−O bond formation step.

B3LYP.[10,11] The advantage of theoretical methods is the relative ease with which different oxidation states and electronic configurations can be studied. DFT with a hybrid functional, e.g., B3LYP, is the only theoretical method with sufficient accuracy that can treat the large models required in this study.

Assuming that a formal Mn^V-oxo state is involved in O−O bond formation, the calculated electronic structure of the synthetic complex with this oxidation state is compared to the electronic structure of the other known active Mn-complex, the OEC in PSII. These two active complexes are then compared to two inactive Mn^V-oxo complexes, trying to find a dividing factor between active and inactive complexes. The O−O bond formation reaction for the synthetic complex is then studied in detail. This is required to show that the O−O bond can form from water with a reasonable barrier. A good match between the experimental and calculated barrier would support the conclusion that the synthetic complex really can be regarded as a reasonable model of the OEC.

In their paper, Limburg et al. propose a reaction scheme for oxidation of water by the synthetic Mn-dimer.[6] In that scheme, which is outlined in Figure 1, the active Mn-dimer is oxidized by the oxygen-atom transfer reagent oxone (HSO_5^-), from a Mn^{IV}-Mn^{III} state to a Mn^{IV}-Mn^V-oxo state. After formation of the Mn^V-oxo intermediate, the oxo group in this intermediate can form O_2 by reacting with either water or oxone. The measured V_{max} for O_2 formation is 2420 ± 490 mol O_2 h^{-1} mol^{-1}. Using transition state theory, this roughly corresponds to a reaction barrier of 18 kcal/mol. By performing the reaction with oxone containing the ^{16}O isotope and water labeled with the ^{18}O isotope, O−O bond formation with water can be distinguished from the competing reaction with oxone. The results are complicated by exchange between water and the oxo group in the intermediate, and the relative amounts of $^{32}O_2$, $^{34}O_2$, and $^{36}O_2$ are not fully consistent with the reaction scheme presented in ref 6. However, even if a numerical correction has to be introduced, it seems clear that O_2 formation with water really does occur and that this reaction has a barrier that is 1−3 kcal/mol higher than the barrier for O_2 formation with oxone.

This theoretical study covers the step in the catalytic cycle shown in black in Figure 1, i.e., the actual O−O bond formation step. In the present investigation, the electronic structure of the highly oxidized intermediate is studied in detail but not its formation. Furthermore, only O−O bond formation with water is modeled, not the same reaction with oxone. One reason for not studying the two oxone reactions is that the major task is to find similarities between this complex and the OEC, and for this purpose the reactions with oxone are not relevant. Other reasons are problems encountered when modeling the negative oxone close to the positive complex. In the calculations, the HOMO in the oxone is an orbital with a positive eigenvalue, indicating that the electronic configuration of the total system is not well described.

When comparing the theoretically calculated barrier for O−O bond formation to the experimentally determined barrier, it should be noted that according to Limburg et al. it is the formation of the Mn^V-oxo intermediate that is the rate-limiting step of the reaction, a step that is not modeled in this study. This means that the barrier for O_2 formation with oxone must be lower than 18 kcal/mol and the barrier for O_2 formation with water should be lower than 19−21 kcal/mol.

The O_2 evolution reaction in the OEC has previously been treated theoretically at different levels of theory. A previous B3LYP study of a model of the OEC suggested an oxygen radical mechanism.[12,13] In that mechanism, the highly oxidized Mn^V-oxo state never appears; instead, a Mn^{IV}-oxyl radical is formed in S_3. The Mn^{IV}-oxyl radical state has the same formal oxidation state as the Mn^V-oxo state but a different electronic configuration. This radical state was found to be active in O−O bond formation, at least in that model of the OEC. Another B3LYP study treating a simpler Mn-dimer model also found that oxidation of a $Mn^{IV}(\mu\text{-}O)_2$-Mn^{IV} species oxidizes an oxygen to a radical rather than any of the Mn^{IV} species to Mn^V.[14]

II. Computational Details

All calculations in this investigation were made using the DFT hybrid functional B3LYP.[10,11] The B3LYP functional can be written as

$$F^{\mathrm{B3LYP}} = (1-A)F_x^{\mathrm{Slater}} + AF_x^{\mathrm{HF}} + BF_x^{\mathrm{Becke}} + CF_c^{\mathrm{LYP}} + (1-C)F_c^{\mathrm{VWN}}$$

where F_x^{Slater} is the Slater exchange, F_x^{HF} is the Hartree−Fock exchange, F_x^{Becke} is the gradient part of the exchange functional of Becke, F_c^{LYP} is the correlation functional of Lee, Yang, and Parr,[15] and F_c^{VWN} is the correlation functional of Vosko, Wilk, and

(10) Becke, A. D. *J. Chem. Phys.* **1993**, *98*, 1372−1377.
(11) Becke, A. D. *J. Chem. Phys.* **1993**, *98*, 5648−5652.
(12) Siegbahn, P. E. M. *Inorg. Chem.* **2000**, *39*, 2923−2935.
(13) Siegbahn, P. E. M. *Curr. Opin. Chem. Biol.* **2002**, *6*, 227−235.
(14) Aullón, G.; Ruiz, E.; Alvarez, S. *Chem. Eur. J.* **2002**, *8*, 2508−2511.
(15) Lee, C.; Yang, W.; Parr, R. G. *Phys. Rev. B* **1988**, *37*, 785−789.

Nusair.[16] *A*, *B*, and *C* are the coefficients determined by Becke using a fit to experimental heats of formation, where the correlation functionals of Perdew and Wang[17] were used instead of F_c^{VWN} and F_c^{LYP} in the expression above. The accuracy of the B3LYP method has been estimated using several benchmark tests, most recently the extended G3 set (376 entries). Including only the 301 entries that are most relevant when only a few bonds are formed or broken, the B3LYP functional has an average error of 3.29 kcal/mol.[18]

It has been claimed that the B3LYP functional favors high spin states over low spin states. As seen in the definition above, the B3LYP functional contains an HF exchange term. In HF calculations, high spin states are favored since contributions from Fermi correlation are included in the calculation of exact exchange while contributions from Coulomb correlation are not. Recently, it has been suggested that the energy splitting between different spin states in an iron complex is more accurately described if the coefficient in front of the HF exchange term in the B3LYP expression (A in the B3LYP formula above) is decreased from 0.20 to 0.15.[19] This modification of the functional has been used when investigating the ground state of the oxidized complex and to calculate modified reaction barriers.

The coordinates of the Mn-complex were obtained from the Cambridge Crystallographic Data Centre as entry CCDC 113788.[20] The crystallized complex is in the $Mn^{IV}-Mn^{III}$ oxidation state, but in the X-ray structure the two Mn-atoms appear to be identical since they are on inversion centers. Despite the difference in oxidation states, the X-ray structure is used as a starting point for the optimization of the oxidized $Mn^{IV}-Mn^{V}$ state.

The oxidized complex consists of 66 atoms, out of which 44 are heavy atoms. A full model of the oxidized complex, in this paper referred to as the large model, is shown in Figure 2. To decrease the computational effort, especially for Hessian calculations, the complex was modeled by 42 atoms by removing parts of the terpyridine ligands. This model, in this paper referred to as the small model, is shown in Figure 3. Most of the results reported in this paper are obtained using the small model. The large model has only been used to add corrections to the energy profile for the O_2 formation reaction, originally calculated using the small model.

Some changes occur when going from the large to the small model. Mulliken spin populations change by 0.10 and less, and the core Mn−O distances change by up to 0.04 Å. Selected distances and spin populations for the oxidized form of the two models are shown in Table 1. The relative energies of different spin states are also affected to a minor extent. In both models, there is significant spin on oxygen (O3 in Figure 2). In the large model, the state where the spin on O3 is aligned antiparallel with the spin on the closest Mn (Mn2) lies 4.7 kcal/mol (lacvp basis set only) below the state where the spins on O3 and Mn2 are parallel. In the small model, the corresponding value is 5.6 kcal/mol. The error of 0.9 kcal/mol when using the small model is considered tolerable when discussing energy differences between different spin states.

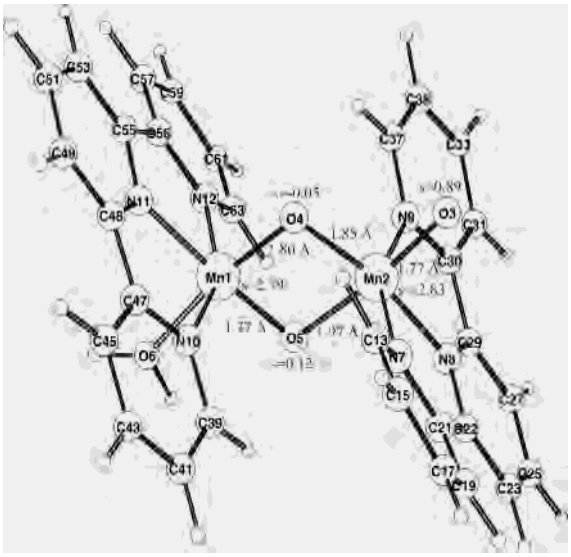

Figure 2. Optimized structure (full model) of the oxidized state of the active complex [(terpy)(H_2O)Mn^{IV}(μ-O)$_2$$Mn^{IV}$($O^{\bullet}$)(terpy)]. Distances are given in Å, and spins are taken from Mulliken spin populations using the lanl2dz basis set.

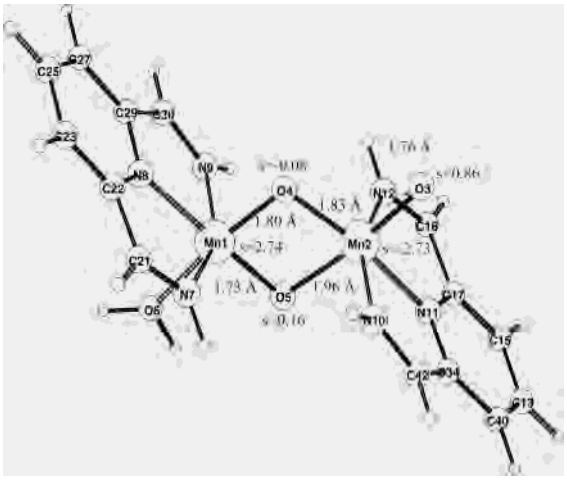

Figure 3. Optimized structure of a small model of the active complex in the oxidized state. Compared to the large model of the complex, parts of the terpyridine ligands have been removed. The maximum difference between the small and the large complex is 0.10 for spin populations and 0.04 Å for distances. Distances are given in Å, and spins are taken from Mulliken spin populations using the lanl2dz basis set.

The calculation of the activation barrier involves finding a fully optimized transition state, and for this purpose a Hessian calculation is required. To enable these calculations in a reasonable time, the small complex is used in the calculation of the reaction energy profile. Solvent, large basis, zero point, and thermal effects are all calculated using the small model. In the calculations of the O_2 formation reaction with water, a minor problem occurs in the small model. The water molecule participating in the O−O bond formation forms an artificial hydrogen bond to an N−H proton that does not exist in the large model of the complex. To correct for this error and possibly other errors resulting from the use of a small model, the large model is used in optimizations with the reaction coordinates frozen from the smaller model. Single point calculations with the modified B3LYP functional proposed by Reiher et al.[19] are used to estimate the sensitivity of the calculated barriers to the functional form.

(16) Vosko, S. H.; Wilk, L.; Nusair, M. *Can. J. Phys.* **1980**, *58*, 1200.
(17) Perdew, J. P.; Wang, Y. *Phys. Rev. B* **1992**, *45*, 13244−13249. Perdew, J. P. In *Electronic Structure of Solids*; Ziesche, P., Eischrig, H., Eds.; Akademie Verlag: Berlin, 1991. Perdew, J. P.; Chevary, J. A.; Vosko, S. H.; Jackson, K. A.; Pederson, M. R.; Singh, D. J.; Fiolhais, C. *Phys. Rev. B* **1992**, *46*, 6671−6687.
(18) Curtiss, L. A.; Raghavachari, K.; Redfern, R. C.; Pople, J. A. *J. Chem. Phys.* **2000**, *112*, 7374−7383.
(19) Reiher, M.; Salomon, O.; Hess, B. A. *Theor. Chem. Acc.* **2001**, *107*, 48−55.
(20) Limburg, J.; Vrettos, J. S.; Liable-Sands, L. M.; Rheingold, A. L.; Crabtree, R. H.; Brudvig, G. W. *Science* **1999**, *283*, 1524−1527.

Table 1. Selected Core Distances and Mulliken Spin Populations for the Large and the Small Model of the Oxidized Form of the Active Mn-Dimer[a]

	spin population					distance (Å)		
	Mn1	Mn2	O3	O4	O5	Mn2−O3	Mn2−O4	Mn2−O5
large complex	2.79	−2.83	0.89	−0.05	0.12	1.77	1.85	1.97
small complex	2.74	−2.73	0.86	−0.08	0.16	1.76	1.83	1.96

[a] Spin populations are calculated with the lanl2dz basis set.

Geometries are optimized using a double-ζ basis set, either the lanl2dz or the lacvp basis set. The lanl2dz basis set is a d95 basis set[21] with a nonrelativistic ECP (effective core potential)[22] for the manganese atoms. The lacvp basis set uses the same ECP but is based on the 6-31G basis set. Optimization with a small basis set has been shown to be sufficient since the final energy is rather insensitive to the quality of the geometry optimization.[23] The lanl2dz basis set is used for the Hessian calculations. Optimized equilibrium structures are accepted if the Hessian only has positive eigenvalues. Transition states (TS) are also obtained by full optimizations and are characterized by a single negative eigenvalue of the Hessian. The Hessians are also used to estimate zero-point, thermal, and entropy effects on the relative energies. Following the geometry optimization, the electronic energy is calculated using the lacv3p** basis set with polarization functions added to all atoms. The lacv3p basis set is of triple-ζ quality and uses an ECP[22] for the manganese atoms. The calculations in this investigation are performed with the programs Jaguar[24] and Gaussian98.[25]

The part of the solvent that is not explicitly included in the model is treated as a homogeneous medium with a dielectric constant of 80, to mimic the properties of solvent water. All solvent corrections are calculated using the Poisson−Boltzmann solver in Jaguar.[26]

Finally, DFT does not correctly describe the spin-coupling in open shell antiferromagnetic states. To be able to correct the energy of the low-spin state, states with both the highest and lowest M_s values should be calculated. A *J*-value can then be obtained using the Heisenberg Hamiltonian formalism.[27] In principle, the correction should be applied to all states with antiferromagnetic coupling. The *J*-value for the two high-spin Mn^{IV}-centers in the active species (see Figure 3) is calculated to be 0.67 kcal/mol, and the *J*-value correction for the splitting between ferro- and antiferromagnetically coupled dimers is 0.99 kcal/mol. The correction is almost the same (1.01 kcal/mol) if the second center also includes the spin on the oxyl radical. In the present study, it is assumed that the correction for antiferromagnetic coupling between the two Mn-centers stays approximately constant during the reaction studied. A *J*-value correction is also calculated between a high spin Mn^{IV}-center and an oxyl radical. The calculated *J*-value is 3.74 kcal/mol, and the *J*-value correction for the splitting between the parallel and antiparallel spin solution is calculated to be 1.87 kcal/mol. This value is included in the energy difference between the active species with low spin and the active species with high spin. It is assumed that this correction does not change significantly during the redox reaction either. No separate *J*-value corrections have been performed for transition states and intermediates.

III. Results

IIIa. Electronic Structure of the Highly Oxidized Complex. The present investigation largely follows the reaction scheme proposed by Limburg et al.[6] They suggested that the active species in O−O bond formation for the synthetic complex is the Mn^{IV}-Mn^{V}-oxo state. In principle, there exists a large number of different spin states for a complex with these formal oxidation states, and the first computational task is to identify the electronic structure of the state with the lowest energy.

To simplify the discussion, the formal Mn^{V}-oxo species is first discussed separately, without including the second Mn center of the dimer. A Mn^{V} ion has two electrons in the 3d-orbital, making up a possible low spin singlet state, termed S1, and a high spin triplet state, termed T1. These two states, and other spin states for the formal Mn^{V}-oxo species, are shown schematically in Figure 4. Starting from T1, an alternative triplet state can be formed if one of the bonding electron pairs between manganese and oxygen is split, with one electron going to Mn, which becomes Mn^{IV}, and the other to oxygen, which becomes an oxyl radical. This state is termed T2. The difference compared to the first triplet state T1 is in the distribution of unpaired spins on Mn and O, as indicated by their Mulliken spin populations. The Mn−O bond distance is also longer in the radical triplet since the Mn−O bond order is reduced. From this triplet radical state T2, the spin on the oxyl radical can be reversed to make it parallel to the three spins on Mn^{IV} giving a total of four parallel spins, i.e., a quintet, termed Q.

In an analogous fashion, an oxyl radical state S2 can be formed from the low spin singlet state S1, if the oxyl spin is antiparallel to the spin on Mn^{IV} and a triplet state T3 if the spins are parallel. All these states are shown in Figure 4.

In the Mn-dimer, the six different spin states of the formal Mn^{V}-oxo species combine with the spin of three 3d electrons of the other Mn^{IV} ion in the dimer. The Mn^{IV} ion can form a low spin and a high spin state, and the two Mn ions can couple either ferromagnetically or antiferromagnetically. This gives a total of 24 different spin states for the dimer.

(21) Dunning, T. H., Jr.; Hay, P. J. In *Methods of Electronic Structure Theory, Modern Theoretical Chemistry*; Schaefer, H. F., Ed.; Plenum Press: New York, 1976; Vol. 3, pp 1−28.
(22) Hay, P. J.; Wadt, W. R. *J. Chem. Phys.* **1985**, *82*, 299−310.
(23) Siegbahn, P. E. M. In *New Methods in Computational Quantum Mechanics, Advances in Chemical Physics*; Prigogine, I., Rice, S. A., Eds.; Wiley-Interscience: New York, 1996; Vol. XCIII, pp 333−387.
(24) Jaguar 4.1; Schrödinger Inc.: Portland, OR, 1991−2000.
(25) Frisch, M. J.; Trucks, G. W.; Schlegel, H. B.; Scuseria, G. E.; Robb, M. A.; Cheeseman, J. R.; Zakrzewski, V. G.; Montgomery, J. A., Jr.; Stratmann, R. E.; Burant, J. C.; Dapprich, S.; Millam, J. M.; Daniels, A. D.; Kudin, K. N.; Strain, M. C.; Farkas, O.; Tomasi, J.; Barone, V.; Cossi, M.; Cammi, R.; Mennucci, B.; Pomelli, C.; Adamo, C.; Clifford, S.; Ochterski, J.; Petersson, G. A.; Ayala, P. Y.; Cui, Q.; Morokuma, K.; Malick, D. K.; Rabuck, A. D.; Raghavachari, K.; Foresman, J. B.; Cioslowski, J.; Ortiz, J. V.; Stefanov, B. B.; Liu, G.; Liashenko, A.; Piskorz, P.; Komaromi, I.; Gomperts, R.; Martin, R. L.; Fox, D. J.; Keith, T.; Al-Laham, M. A.; Peng, C. Y.; Nanayakkara, A.; Gonzalez, C.; Challacombe, M.; Gill, P. M. W.; Johnson, B. G.; Chen, W.; Wong, M. W.; Andres, J. L.; Head-Gordon, M.; Replogle, E. S.; Pople, J. A. *Gaussian 98*; Gaussian, Inc.: Pittsburgh, PA, 1998.
(26) Tannor, D. J.; Marten, B.; Murphy, R.; Friesner, R. A.; Sitkoff, D.; Nicholls, A.; Ringnalda, M.; Goddard, W. A., III; Honig, B. *J. Am. Chem. Soc.* **1994**, *116*, 11875−11882.
(27) Noodleman, L.; Case, D. A. *Adv. Inorg. Chem.* **1992**, *38*, 423−470.

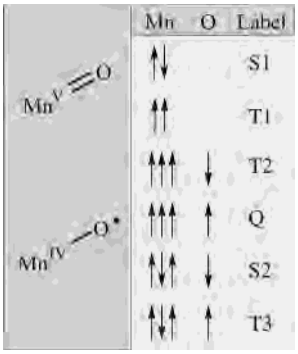

Figure 4. Possible spin states for a formal Mn^{V}-oxo species when oxyl radical states are considered. Arrows symbolize unpaired electrons. The spin state labels are those referred to in the text.

Table 2. Nine Possible Spin States for the Formal $Mn^{IV}-Mn^{V}$ Dimer, Including Oxyl Radical States[a]

		formal spin			Mulliken spin			relative energy
no.	multiplicity	Mn1	Mn2	O3	Mn1	Mn2	O3	(kcal/mol)
1	doublet	3	−3	1	2.73	−2.73	0.85	0.00
2	sextet	3	3	−1	2.72	2.73	−0.80	+3.04
3	doublet	−3	3	1	−2.79	2.55	1.20	+5.62
4	octet	3	3	1	2.71	2.63	1.23	+10.04
5	quartet	3	−1	1	2.60	−0.52	0.83	+11.90
6	doublet	−1	3	−1	1.51	2.68	−0.77	+19.77
7	quartet	3	1	−1	2.71	1.01	−0.55	+20.00
8	quartet	1	3	−1	0.77	2.63	−0.77	+20.55
9	doublet	1	−1	1	1.65	−0.47	−0.90	+26.13

[a] Other spin states exist but are believed to be higher in energy than at least the first eight. Energies and spin populations are obtained after full geometry optimizations of the small model (Figure 3) using the lacvp basis set. Energies do not include *J*-value corrections or corrections for solvent, zero-point, and thermal effects. Formal spins with integral numbers are assigned to facilitate the rationalization of the different spin states.

However, not all these states appear as minima on the potential energy surfaces if the structures are geometry optimized. As an example, for a Mn^{V}-oxo species, the triplet state with high spin on Mn (T1 in Figure 4) is converted into the Mn^{IV}-oxyl radical state (T2 in Figure 4) without an energy barrier upon geometry optimization. After this consideration, there are still 16 different spin states for the dimer. Table 2 lists nine of these. The missing spin states have low spin on one or both Mn atoms and should therefore have a higher energy than at least the first eight states in Table 2.

From the relative positions of the different spin states in Table 2, two rules can easily be observed. As expected, the spins on two neighboring centers are preferably antiparallel, and high spin is preferred over low spin on an individual center. Accordingly, the most stable state is an antiferromagnetically coupled dimer with two high spin Mn^{IV} and an oxyl radical on the terminal oxygen with its spin antiparallel to the closest Mn. The Mulliken spin population on oxygen is not exactly 1.0 but 0.85 (lacvp basis set). However, this is definitely more radical than oxo character, and the species will be termed an oxyl radical throughout the text. The spin on the closest Mn is −2.73, which is close to the expected spin for a Mn^{IV} ion. These calculations therefore indicate that the active state of the synthetic complex is a Mn^{IV}-oxyl radical state and not a Mn^{V}-oxo state, as proposed by Limburg et al.

Table 3. Mulliken Spin Populations for the Small Model of the Reactant in the O−O Bond Formation Reaction[a]

	atom labels from Figure 3					
calculation	Mn1	Mn2	O3	O4	O5	O6
basic model	2.74	−2.73	0.86	−0.08	0.16	0.00
modified functional	2.66	−2.58	0.75	−0.07	0.17	0.00
neutral model	2.72	−2.65	0.84	−0.13	0.17	0.00
solvent	2.76	−2.74	0.84	−0.07	0.14	0.01
large basis	2.80	−2.77	0.82	−0.06	0.15	0.00

[a] The model has been modified to test the amount of radical character on the oxyl radical (O3 in Figure 3). Spin populations are calculated with the lanl2dz basis set, except for the solvent calculation where the basis set is lacvp and the large basis calculation where the basis set is lacv3p**.

Testing the Oxyl Radical State. Studying the states in Table 2 more carefully, there is not a single Mn^{V}-oxo state. All Mn^{V}-oxo states are on the same spin surface as a Mn^{IV}-oxyl radical state, and if the structures are fully optimized the most stable of the two in all these cases is the oxyl radical state. However, it is possible to get more oxo character by restricting the Mn−O distance. In the fully optimized complex, the Mn−O distance is 1.76 Å (see Figure 3). If the Mn−O bond length is frozen to 1.60 Å, the spin on oxygen drops from 0.86 to 0.56 (lanl2dz basis set), but the energy increases by 5.4 kcal/mol. Shorter bond lengths increase the energy further and when the restricted structures are released, they return to the Mn^{IV}-oxyl radical state with a bond distance of 1.76 Å. In the present calculations the oxyl radical state is clearly the most stable for this complex.

It could be argued that the present method and model have a tendency to overestimate the radical character and that the oxyl radical therefore is an artifact of the method. Since the results of the present investigation suggest that the formation of an oxyl radical is a requirement for O−O bond formation, it is important to analyze the situation further. Therefore, several tests of both method and model have been performed. They are all described below, and the effects of the modifications on the Mulliken spin population of the oxyl radical species are summarized in Table 3.

Test 1. As discussed in the Computational Details section, it has been claimed that the B3LYP functional favors high spin states over low spin states due to the effect of the HF exchange term. Changing the coefficient in front of the HF exchange term in the B3LYP expression (*A* in the B3LYP formula in the Computational Details section) from 0.20 to 0.15, as proposed by Reiher et al.,[19] would decrease the tendency of the calculations to show radical character for the terpyridine complex. If the structure is reoptimized with the modified functional, the spin on oxygen decreases from 0.86 to 0.75, but this is still a significant radical character on oxygen. At the same time, the Mn−O distance decreases slightly (from 1.76 to 1.73 Å). These results can further be compared with calculations without any contribution from HF exchange. If the HF exchange contribution is set to 0.0 in a modified B3LYP functional, the spin population on oxygen is 0.45 for the original B3LYP geometry but drops to −0.25 (parallel to the spin on Mn) during geometry optimization. At the same time, the Mn−O distance decreases to 1.62 Å. The nonhybrid BLYP functional gives a spin population of 0.50 on oxygen for the original B3LYP

geometry. During geometry optimization, this spin population drops to −0.07, and the Mn−O distance becomes 1.64 Å.

There are thus significant differences between results with and without contributions from HF exchange. However, benchmark tests consistently show that the hybrid functional B3LYP performs better compared to the nonhybrid BLYP functional. In the benchmark test described in the Computational Details section, the mean absolute deviation is 3.29 kcal/mol for B3LYP and 6.17 for BLYP. Looking at all 376 entries in the G3/99 test, the mean absolute deviation is 4.27 kcal/mol for B3LYP and 7.60 for BLYP. A relevant example for Mn is the calculation of the terminal O−H bond strength of the permanganate ion $MnO_3(OH)^-$. The estimated bond strength from experiment is 80 ± 3 kcal/mol.[28] B3LYP gives a reasonable result of 77.2 kcal/mol while BLYP gives an O−H bond strength of 59.5 kcal/mol, approximately 20 kcal/mol lower than the experimental value.[29]

Test 2. The nominal charge of the complex is +3, and since counterions are not included, the computational model has the unusually high charge of +3. This positive charge creates a strong Coulomb attraction that may attract peripheral electrons, thus creating artificial radicals. This could be the case for the radical Mn^{IV}-oxyl state, where an electron has moved from a terminal bond to the highly charged Mn ion. To test this, three negative counterions were added to the model. In the computational model, Cl^- ions were chosen as counterions instead of the NO_3^- ions as in the experiments. After optimization, one Cl^- ion is hydrogen bonded to the water molcule (O6 in Figure 3) while the other two are hydrogen bonded to amide protons (at N9 and N12 in Figure 3). In the neutral model, the spin on oxygen is almost unchanged compared to the charged model, 0.84 compared to 0.86.

Test 3. Using a similar argument as above, a gas phase calculation does not shield the electrostatic interactions properly and may therefore favor the Mn^{IV}-oxyl state compared to the Mn^V-oxo state. The complex was therefore reoptimized in a water solvent, treated as a homogeneous dielectric medium. This treatment does not change the spin on oxygen significantly; the Mulliken spin population of the oxyl radical in a water solvent is 0.84 (lacvp basis set).

Test 4. The double-ζ basis set is a rather small basis set, and it can be argued that increasing the number of basis functions on each atom might increase the ability of oxygen to keep a high partial negative charge. However, a single point calculation using the larger lacv3p** basis set did not show any significant change in the Mulliken spin population on oxygen (Mulliken spin of 0.82).

From these results, summarized in Table 3, it is clear that the amount of unpaired spin on oxygen is rather independent of the model. Together, the results suggest that the active synthetic complex is better described as a Mn^{IV}-oxyl radical state than as a Mn^V-oxo state.

Inactive Mn^V-Oxo Complexes. The preference for an oxyl radical state over a Mn^V-oxo state seems to be a common feature of the present terpyridine model complex and different models of the OEC in B3LYP calculations.[12,14] To test if the B3LYP treatment always leads to a preference for the oxyl radical state, independent of the type of Mn-complex, the attention was turned to some experimentally well characterized Mn^V-oxo complexes, known to be low spin d^2. Two of these Mn^V-oxo complexes, known to be inactive in O_2 formation, were selected for investigation.[7,9]

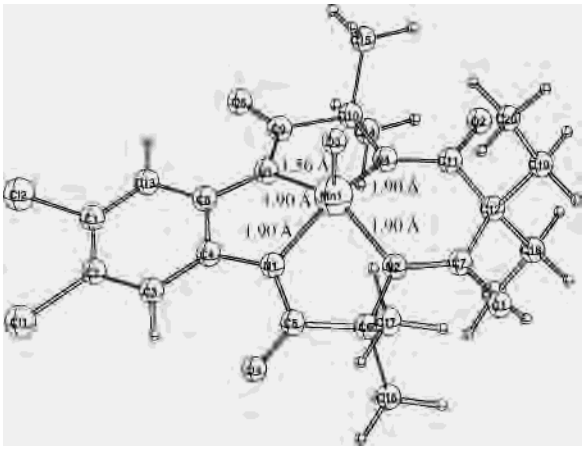

Figure 5. Mn^V-oxo complex inactive in O_2 formation.[7] It has a tetraamide ligand and square pyrimidal coordination. Distances are given in Å. The computed distances agree well with those determined from X-ray structures. The most stable state is a closed shell singlet state, in full agreement with experiment.

The first inactive complex investigated has a tetraamide ligand, forming a square pyramidal Mn^V-oxo complex (see Figure 5).[7] The second one has a bis-amido bis-alkoxo ligand, and the geometry is again square pyramidal (see Figure 6).[9] Apart from information about the ground state, which in both cases is known to be low spin, the X-ray structures of the two complexes are also available.

In these cases, the computational results can be compared to reliable experimental data for geometry and spin states, a possibility that does not exist for the two active complexes, the OEC and the synthetic complex investigated in the present study. The investigation also makes it possible to compare the results for active and inactive complexes, and find differences between the two types of complexes that can help to understand the mechanisms for O−O bond formation.

As discussed above, the possible spin states for a nominal Mn^V-oxo species, if oxyl radical states are included, are singlet, triplet, and quintet. First, for the complex with the tetraamide ligand, the singlet (low spin d^2) Mn^V-oxo state is the most stable, in agreement with experiment. The calculated Mn−O distance is 1.559 Å, which is in good agreement with the experimental distance of 1.555 Å. This is much shorter than the 1.76 Å calculated for the Mn−O bond length in the active terpyridine complex. The results are summarized in Table 4.

A triplet state is found 13.1 kcal/mol above the singlet. However, in contrast to the active complex, the triplet state is still mainly a Mn^V-oxo state, as seen by the relatively low Mulliken spin population of the oxygen (−0.23). The increase in Mn−O bond length is small, going from 1.559

(28) Gardner, K. A.; Mayer, J. M. *Science* **1995**, *269*, 1849−1851.
(29) Siegbahn, P. E. M.; Blomberg, M. R. A. *Annu. Rev. Phys. Chem.* **1999**, *50*, 221−249.

Table 4. Relative Energies, Selected Distances, and Spin Populations of Singlet, Triplet, and Quintet States for Two Inactive Mn^V-Oxo Complexes Experimentally Known to Be Low Spin Singlets[a]

		spin population						distance (Å)					energy
ligand	multiplicity	Mn1	O3	N1	N2	N3	N4	Mn1−O3	Mn1−N1	Mn1−N2	Mn1−N3	Mn1−N4	(kcal/mol)
tetraamide	singlet	0.00	0.00	0.00	0.00	0.00	0.00	1.56	1.90	1.90	1.90	1.90	0.0
tetraamide	triplet	1.97	−0.23	0.03	0.03	0.07	0.07	1.63	1.92	1.92	1.90	1.90	13.1
tetraamide	quintet	2.57	0.72	0.11	0.11	0.08	0.08	1.73	1.93	1.93	1.89	1.89	19.5

		spin population						distance (Å)					energy
ligand	multiplicity	Mn1	O5	N1	N2	O3	O4	Mn1−O5	Mn1−N1	Mn1−N2	Mn1−O3	Mn1−O4	(kcal/mol)
bis-alkoxo bis-amido	singlet	0.00	0.00	0.00	0.00	0.00	0.00	1.56	1.89	1.89	1.83	1.83	0.0
bis-alkoxo bis-amido	triplet	2.04	−0.16	−0.06	0.01	0.12	0.02	1.62	1.90	1.94	1.84	1.80	4.3
bis-alkoxo bis-amido	quintet	2.50	0.79	0.05	0.16	0.15	0.02	1.74	1.93	1.94	1.84	1.85	12.4

[a] See refs 7 and 9. Labels refer to Figures 5 and 6, respectively. Distances and Mulliken spin populations are obtained after optimizations using the lacvp basis set. Relative energies are calculated with the lacv3p** basis set and include solvent effects.

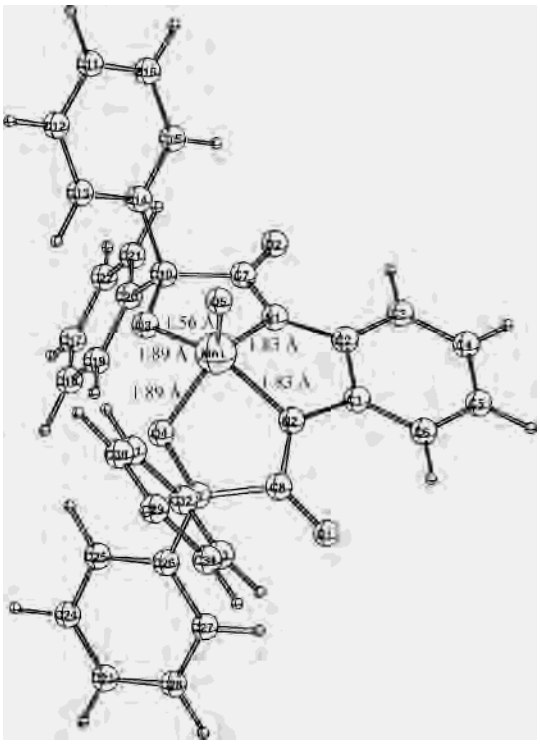

Figure 6. Mn^V-oxo complex inactive in O_2 formation.[9] It has a bis-alkoxo bis-amido ligand and square pyrimidal coordination. Distances are given in Å. The computed distances agree well with those determined from X-ray structures. The most stable state is a closed shell singlet state, in full agreement with experiment.

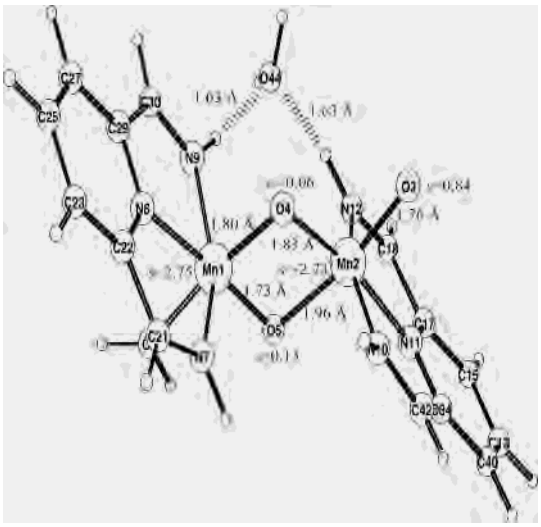

Figure 7. Model reactant for O−O bond formation. Note that, in this model, the water molecule accepts two hydrogen bonds from the ligand, but these hydrogen bond donors are not present in the large model of the complex. Distances are given in Å, and spins are taken from Mulliken spin populations using the lanl2dz basis set.

to 1.563 Å. The oxyl radical state appears first for the quintet state (Mulliken spin on oxygen of 0.72), but this state lies 19.5 kcal/mol above the singlet. The Mn−O distance is 1.726 Å, which is similar to the oxyl radical state in the active complex.

The results for the second Mn^V-oxo complex with a bis-alkoxo bis-amido ligand (see Figure 6) are similar to the results presented above. Splittings between energy levels, bond distances, and Mulliken spin populations differ slightly, for details see Table 4, but the low spin Mn^V-oxo is clearly the most stable one, in agreement with experiment. For these complexes, there seems to be agreement between experimental and computational data. The results also show that a B3LYP treatment is able to give a Mn^V-oxo species and does not always prefer a radical species.

IIIb. O−O Bond Formation with Water. Before discussing similarities between the OEC and the oxyl radical state in the synthetic complex, it must be shown that this radical species actually is an active intermediate in the O_2 formation reaction with water. The computational task is therefore to determine the activation barrier for the O−O bond formation reaction.

In the reaction, a water molecule, or possibly a hydroxide ion, should form an O−O bond with the oxyl radical of the complex. A single water molecule was therefore added to the small model of the terpyridine complex (see Figure 7). During the O−O bond formation reaction, the water molecule must lose one of its protons to a base. In the computational model, the base is one of the bridging oxygens (O4 in Figure 7). During the reaction the Mn having an oxyl ligand (Mn2) receives an electron from the oxyl radical and is reduced to Mn^{III}.

The previous analysis of the different spin states of the active species showed that the three spins on Mn^{IV} and the spin on the oxyl radical are preferably antiparallel, together forming a triplet state. Note that the spin of the second Mn (Mn1 in Figure 7) does not change during this reaction and

these spins are therefore not included in this discussion. If the electron is transferred from the oxyl radical to the active Mn, this results in a triplet Mn^{III}. However, it can be expected that Mn^{III} with its d^4 configuration prefers to form a high spin quintet state. The low energy reactant, which has antiparallel spin between the three electrons on Mn^{IV} and the electron on the oxyl radical, is thus not directly electronically connected to the most stable product, where the spins of these four electrons are parallel.

The more stable high spin product can be reached by spin flipping in the triplet Mn^{III} product. Another alternative reaction path is to start from the excited high spin reactant, where the three spins on Mn^{IV} and the spin on the oxyl radical are already parallel, and perform the reaction from this species.

As mentioned above, the spectator Mn (Mn1 in Figure 7) is not considered in the discussion of the two different spin surfaces. It remains high spin Mn^{IV} throughout the reaction, with its spins coupled antiparallel to those on Mn2. The analysis of different spin states in Table 2 shows that any other configuration of the spins on Mn1 results in a higher energy. Since the spins on Mn1 are not believed to have a large influence on the relative energy of the TS compared to the reactant, nothing is gained by adding Mn1 to the discussion. The terms antiparallel and parallel therefore refer only to the spins on the active Mn (Mn2) and the oxyl radical (O3).

The attention is first turned to the reaction on the antiparallel spin surface, starting at the ground state of the reactant. In the large model, the water molecule donates a hydrogen bond to the μ-oxo group in the reactant (see Figure 8). The reaction proceeds by approaching the oxygen of the water molecule (O44) toward the oxyl radical (O3). As the O−O bond is formed, the water molecule must lose one proton. In the model, the proton that initially forms a hydrogen bond to the μ-oxo group (O4) will be transferred to this group. At the same time, Mn (Mn2) is reduced by accepting an electron from the oxyl radical, going from Mn^{IV} to Mn^{III}. In contrast to high spin Mn^{III}, the low spin Mn^{III} that is formed does not have a Jahn−Teller axis so the coordination geometry of Mn^{III} does not change significantly. In the antiparallel reaction that forms a low spin Mn^{III} there are only two major reaction coordinates, the O3−O44 distance and the O−H distance in water. A TS with a single imaginary frequency was found at 23.4 kcal/mol above the reactant, see Figure 9. All effects on the height of the TS barrier are shown in Table 5. The TS appears rather late along the reaction coordinate since, on this spin surface, the reactant is more stable than the product. This is manifested in the short O−O distance, which is as short as 1.69 Å in the TS. The O−H distance is still very short (1.05 Å). At this point, most of the spin has been transferred to Mn2 which has a spin of −2.11 while 0.10 remains on the oxygens, mainly O44. After the TS, triplet Mn^{III} (Mulliken spin of 1.91) is formed 19.1 kcal/mol above the reactant. The Mulliken spin populations of all species are shown in Table 6, and the energy surface is shown in Figure 10. From this low spin product, the spin on Mn^{III} can flip to a high spin

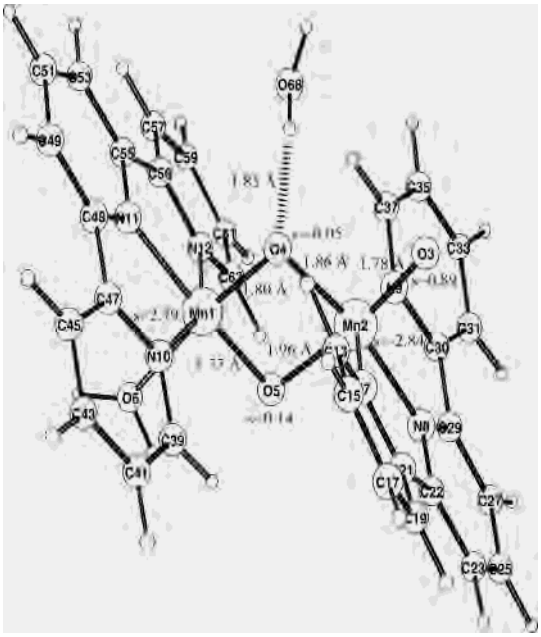

Figure 8. Model reactant for the O−O bond formation using the large model of the complex. This model has been used to calculate corrections to the energy surface obtained by detailed calculations on the small model. The most important difference is the position of the water molecule, now donating a hydrogen bond to the bridging oxo group (O4). Distances are given in Å, and spins are taken from Mulliken spin populations using the lanl2dz basis set.

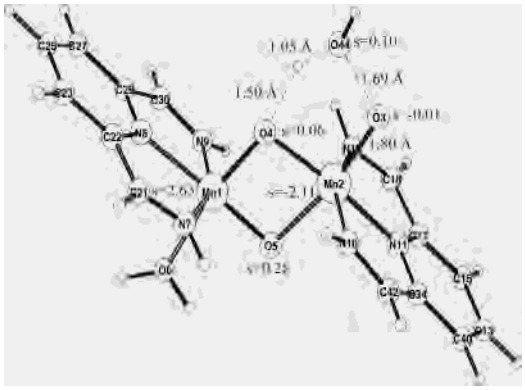

Figure 9. Fully optimized TS for the O−O bond formation reaction on the antiparallel spin surface. The calculated reaction barrier is 23.4 kcal/mol. Distances are given in Å, and spins are taken from Mulliken spin populations using the lanl2dz basis set.

state which is believed to be fast due to a large spin−orbit coupling on the metal.

The alternative reaction path starts with a reactant where the spins on the oxyl radical and the Mn^{IV} are parallel. This spin configuration lies 8.8 kcal/mol higher in energy than the antiparallel reactant. Note that this value includes *J*-value corrections as well as corrections for solvent, zero-point, and thermal effects. The value is therefore slightly different from the one reported in Table 2 which only includes the electronic energy from a small basis set calculation.

Proceeding along the parallel spin surface, Mn^{IV} turns into a high spin Mn^{III}. On this surface, the TS is difficult to find, and one reason for this is that high spin Mn^{III} is Jahn−Teller active. Ligands along the Jahn−Teller axis are

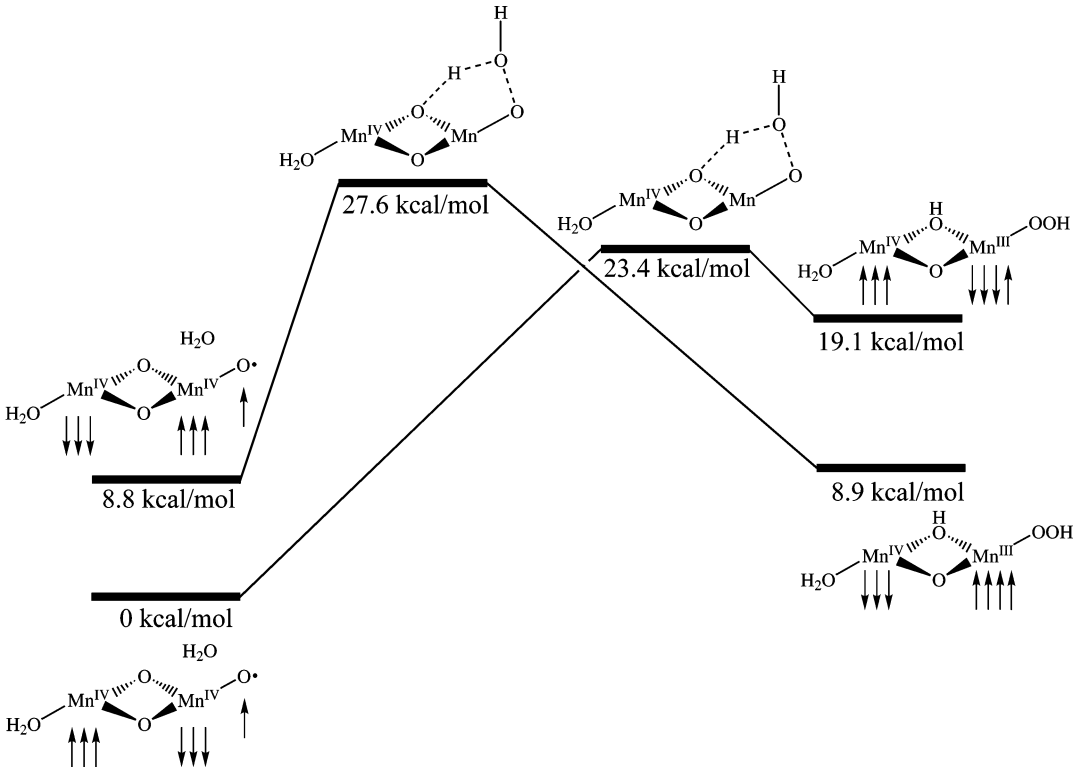

Figure 10. Energy diagram for the O−O bond formation reaction. The two energy surfaces represent the antiparallel and the parallel spin surface, respectively. The location of the crossing between the two spin surfaces has not been determined.

Table 5. Calculated Reaction Barrier for O−O Bond Formation Including Corrections[a]

spin surface	small basis	large basis	solvent	thermal	model size	exchange	*J*-value corr	sum
antiparallel	22.74	+5.39	−0.24	+0.10	−3.14	−1.48	0.00	23.37
parallel	28.35	+0.93	2.04	−3.15	−3.53	+1.07	1.87	27.58

[a] The table shows calculated values for the parallel and the antiparallel spin surface.

Table 6. Mulliken Spin Populations (lanl2dz Basis Set) and Relative Energies for Reactant, TS, Intermediates, and Product Involved in the O−O Bond Formation Reaction

	spin population						energy
	Mn1	Mn2	O3	O4	O5	O44	(kcal/mol)
antiparallel reactant	2.75	−2.73	0.84	−0.06	0.13	0.00	0.0
antiparallel TS	2.63	−2.11	−0.01	0.06	0.28	0.10	23.4
antiparallel product	2.48	−1.91	−0.10	0.04	0.46	0.01	19.1
parallel reactant	−2.79	2.58	1.19	0.03	−0.06	0.00	8.8
parallel TS	−2.60	3.48	0.39	−0.12	−0.28	0.10	27.6
parallel product	−2.47	3.85	−0.06	−0.06	−0.42	0.04	8.9

weakly bonded with very long metal−ligand bond distances. Therefore, the reaction coordinate must include a large change in ligand distances along the Jahn−Teller axis. Simply decreasing the O−O distance and increasing the O−H distance from the reactant does not lead to the desired product, only to a very high energy Mn^{IV} structure. Starting from the product and approaching the reactant leads to a completely different 2D energy surface, now staying at Mn^{III} independent of the O−O and O−H distances. It is necessary to involve several Mn−ligand distances as well to locate the TS. Consideration of the Jahn−Teller axis of the high spin Mn^{III} species is the most important. The Jahn−Teller axis is preferentially aligned to include only the terpyridine ligand. The Mn2−N ligand distance increases from 2.02 Å in the reactant to 2.27 Å in the product Mn^{III} state. This change in ligand distance must be included in the reaction coordinate to find the transition between the reactant and the product 2D energy surfaces. An initial Hessian is then calculated at a geometry where the Mulliken spin is between the values expected for Mn^{IV} and Mn^{III}. From this Hessian, it is possible to locate the TS. In the TS, the Mn−N distance is 2.14 Å (see Figure 11). This TS lies at 27.6 kcal/mol above the antiparallel reactant, and this is higher than the TS on the antiparallel surface. The spin on Mn (Mn2) is 3.48, which is halfway toward Mn^{III}, and a spin of 0.39 remains on the previous oxyl radical (O3). In the TS, the O−O bond is 1.87 Å, which is much longer than for the antiparallel TS. As can be seen in Figure 11, the proton on water shows no tendency to leave for the bridging oxo group in the TS. However, after passing the TS, the hydrogen goes to the bridging oxo group without any barrier during the geometry optimization. The product is the high spin Mn^{III}-OOH product discussed above, see Figure 12. As expected, this state is 10.2 kcal/mol more stable than the low spin product.

The energy profiles of both the parallel and the antiparallel reaction surfaces are shown in Figure 10.

Without inclusion of spin−orbit coupling, there is no connection between the two spin surfaces. However, the

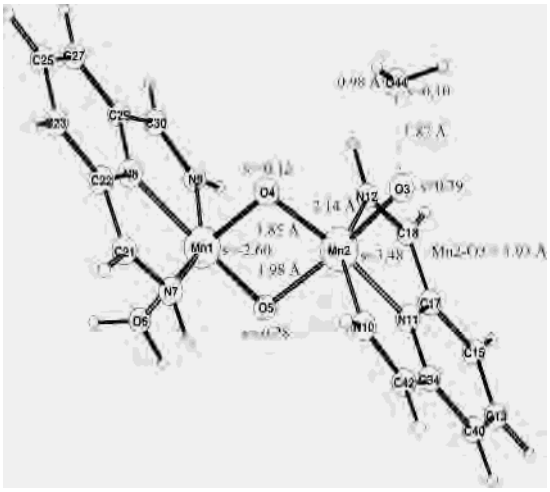

Figure 11. Fully optimized TS for the O−O bond formation reaction on the parallel spin surface. The calculated reaction barrier is 27.6 kcal/mol. Distances are given in Å, and spins are taken from Mulliken spin populations using the lanl2dz basis set.

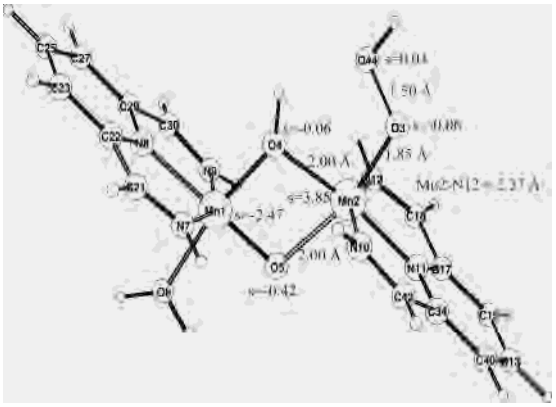

Figure 12. Peroxide product with a high spin Mn^{III}. Note that the Jahn−Teller axis is along the axis that has two nitrogen atoms from the terpyridine ligands. This structure lies 8.9 kcal/mol above the most stable reactant. Distances are given in Å, and spins are taken from Mulliken spin populations using the lanl2dz basis set.

antiparallel spin surface starts below and ends above the parallel one, and it is therefore clear that the two spin surfaces must cross each other at some point. A possibility is that the crossing occurs between the two TS, as indicated in Figure 10. In this case, the path from reactant to product does not have to go through any of the two calculated transition states, and the highest point on the potential energy surface can actually be lower than any of the calculated TS energies. The assumption that the reaction proceeds through the lowest of the two transition states is therefore conservative.

IV. Discussion

The goal of the present investigation was to find the requirements for O−O bond formation in Mn-complexes. The calculations show that the active synthetic complex forms a stable Mn^{IV}-oxyl radical state, the same state that previously was proposed to be the active state in the OEC in photosystem II on the basis of similar calculations.[12] After analyzing and testing some arguments for why the calculations possibly could have an exaggerated tendency to display radical character, the conclusion is that the calculations are expected to give the correct spin distribution of this highly oxidized complex. Although not all these tests have been performed for the model of the OEC, the oxyl radical seems to be a common factor for the two active Mn-complexes. Calculations on the models of the OEC are more uncertain since the relative positions of the Mn-ions are not known and the ligands are unknown. By showing that the same species is involved also in a different complex that is also active in O−O bond formation increases the credibility of the oxyl radical suggestion for the OEC.

The electronic structure of the two active complexes can then be compared to the electronic structures of other Mn^{V}-oxo complexes, known not to be active in O−O bond formation, in order to find a dividing factor between active and inactive complexes. Calculations on two inactive complexes show that they preferably form singlet Mn^{V}-oxo states for the same formal oxidation state as the active complexes form an oxyl radical. The electronic structures of the inactive complexes are in agreement with experiments. These results show that the B3LYP method is able to calculate Mn^{V}-oxo species correctly and that the method does not always give radical states.

There seems to be two major differences between the two inactive Mn^{V}-oxo complexes on one hand and the active Mn-dimer on the other hand. In the inactive complexes, the most stable state has low spin on Mn^{V}. For the Mn-dimer, the state that is closest to this singlet state is state 5 in Table 2. This state has low spin on Mn but lies approximately 12 kcal/mol above the ground state. The inactive complexes investigated also prefer oxo character over oxyl-radical character, both in the singlet and triplet states. In the active complex, both states corresponding to these species form oxyl radicals.

In the inactive complexes, the stability of the Mn^{V}-oxo states is derived from the strong ligand field. The influence of the ligands is also shown in the preference for a low spin d^2 configuration, indicating the presence of a strong ligand field. Furthermore, a Mn^{V}-oxo complex prefers five-coordination because of the strong oxo trans effect. If it is possible, Mn loses its sixth ligand when going from Mn^{IV} to Mn^{V}. However, in the active dimer the terpyridine ligand is tridentate. This constrains the active Mn to a six-coordinated environment, thus favoring a Mn^{IV} state before a Mn^{V} state.

Although the number of investigated Mn-complexes is very limited, a difference between active and inactive complexes can be detected by studying the degree of radical character of the oxo group. It is possible that this degree of radical character, as given by a theoretical calculation, can give information about the possible activity of different complexes, even before synthesis has been attempted. Of course, the calculations give only a limited amount of information and cannot say much about the possibility to synthesize the high oxidation state or the presence of possible side reactions.

Also, concerning the O−O bond formation reaction, the discussion is limited to a formal Mn^{IV}-Mn^{V}-oxo dimer. It can be considered a limitation that the calculations in this paper follow the suggestions from the experimental paper of Limburg et al. and that no other reaction paths or oxidation states have been considered. To prove that this oxyl radical state really is active in O_2 formation, the calculated barrier for O−O bond formation with water is calculated to be 23 kcal/mol or lower, depending on where the spin crossing occurs. The experimental reaction rate corresponds to a total rate-limiting barrier for O−O bond formation with water of 19−21 kcal/mol. If the rate-limiting step is the formation of the active species, not O−O bond formation, the real barrier for O−O bond formation with water must be lower than these 19−21 kcal/mol. The calculated barrier of 23 kcal/mol is therefore slightly too high compared to the experimental result. However, if the error is limited to only 3 kcal/mol, this is within the average error of the method and has to be considered acceptable.

Minor model modifications that would lead to a lower barrier can also be proposed. Possibly, the O−O bond formation reaction could occur with a hydroxide ion instead of water. Taking this into account could result in a lower barrier. A minor problem with the model might be non-optimal steric effects when using a single water molecule both in O−O bond formation and protonation of the bridging oxo group. The location of the water in the reactant might also be a problem although parts of this problem are removed when going to the large model. From the values in Table 5, it can be seen that the effects of going from the small to the large model are not negligible (lowers the barrier by 3 kcal/mol). This effect is not due to a different description of the electronic structure of the core of the complex, but rather in the treatment of the water molecule. In the small model, the water molecule can form hydrogen bonds to amide protons, but these protons are artifacts of the modeling of the complex. These hydrogen bonding possibilities are removed when going to the large model, and this removes the artificial stabilization of the reactant.

Within the present model, a lower activation energy can also be encountered if the crossing point between the parallel and the antiparallel spin surfaces is used to calculate the barrier instead of the lowest of the two transition states.

Since only parts of the reaction have been modeled, the calculated energy profile is based on some assumptions. First, it is assumed that the active complex is stable compared to the complex in the $Mn^{IV}-Mn^{III}$ oxidation state; i.e., no energy is required to form the oxyl radical state from oxone. If there is such an energy penalty, this would add directly to the barrier. Furthermore it is assumed that none of the following steps has a higher barrier than the O−O bond formation step.

The results show that O−O bond formation with water is possible in this complex which supports the conclusion that the synthetic complex really can be regarded as a functional model of the OEC.

V. Summary

B3LYP investigations of a synthetic O_2 catalyst show that this Mn-dimer, as well as models of the oxygen evolving complex, prefers a Mn^{IV}-oxyl radical state rather than a Mn^{V}-oxo state. From this state, O−O bond formation with water occurs with a barrier of 23 kcal/mol. This is a few kcal/mol higher than the experimental estimate but still within the expected uncertainty, and the conclusion is that this reaction is possible. This result supports the suggestion that the active Mn-dimer is a functional model of the OEC.

Calculations on well characterized inactive Mn^{V}-oxo complexes correctly predict that they prefer a singlet Mn^{V}-oxo state. Although the number of investigated complexes is quite limited, it is proposed that radical formation is actually a requirement for O_2 formation in Mn-complexes.

Supporting Information Available: Additional structure files. This material is available free of charge via the Internet at http://pubs.acs.org.

IC0348188